

Check for updates

ORIGINAL ARTICLE

Obesity Biology and Integrated Physiology

Neural Network Dysregulation in Female Abdominal Obesity: Distinct Functional Connectivity in Different Appetite Subtypes

¹Yunnan Key Laboratory of Integrated Traditional Chinese and Western Medicine for Chronic Disease in Prevention and Treatment, Yunnan University of Chinese Medicine, Kunming, China | ²School of Second Clinical Medicine/The Second Affiliated Hospital, Yunnan University of Chinese Medicine, Kunming, China | ³College of Acupuncture and Tuina, Chengdu University of Traditional Chinese Medicine, Kunming, China | ⁴The Sports Trauma Specialist Hospital of Yunnan Province, Kunming, China | ⁵Department of Medical Imaging, The First Affiliated Hospital of Kunming Medical University, Kunming, China

Correspondence: Taipin Guo (gtphncs@126.com) | Yi Lu (lyrix0214@gmail.com)

Received: 13 June 2025 | Revised: 8 August 2025 | Accepted: 12 August 2025

Funding: This work was supported by the "Liang Fanrong Expert Workstation" of Yunnan Province-Yunnan Provincial Science and Technology Plan Project (202305AF150072), the Health Commission of Yunnan Province—Cultivation Objects of High-level Talents in Chinese Medicine in 2023: Acupuncture Discipline Leaders in Chinese Medicine, the Top-Notch Young Talent Project of Yunnan Ten Thousand Talents (YNWR-QNBJ-2019-257), the Priority Union Foundation of Yunnan Provincial Science and Technology Department and Kunming Medical University (202201AY070001-069), and the "Liu Zili Famous Doctor" special talent program of the Yunnan Provincial Xing Dian Talent Support Program (Yunnan Party Talent Office [2022] No. 18).

Keywords: abdominal obesity | appetite subtypes | functional connectivity | independent component analysis | rs-fMRI

ABSTRACT

Objective: This study investigated the neural mechanisms underlying appetite dysregulation in female subjects with abdominal obesity (AO) by identifying functional connectivity (FC) and network-level differences between moderate appetite (MA) and strong appetite (SA) subtypes.

Methods: A total of 60 women with AO (30 MA, 30 SA) and 30 healthy controls (HCs) underwent resting-state fMRI. Independent component analysis was used to identify and examine FC within and functional network connectivity (FNC) between key resting-state networks, including those involved in cognitive and visual processing. Network alterations and correlations with obesity-related indicators were evaluated.

Results: Compared to HCs, both groups showed reduced FC in the default mode network (DMN) and visual network (VN), with SA additionally exhibiting decreased FC in the frontoparietal network (FPN) and lower angular gyrus FC than MA (p<0.05, FDR-corrected). MA displayed increased DMN-left FPN (FPN_L) FNC (p<0.001), while SA showed negative correlations between FC and BMI/appetite visual analog scale (VAS) scores in FPN and with body weight/BMI/appetite VAS in VN (p<0.05). In HCs, DMN-FPN_L FNC positively correlated with BMI, a pattern that was not observed in MA.

Conclusion: Distinct brain network patterns characterize appetite subtypes in AO. SA showed more pronounced FC reductions in networks previously linked to self-regulation and visual processing, which may contribute to appetite dysregulation based on correlations with obesity indicators. In contrast, MA exhibited increased DMN-FPN_L FNC, potentially reflecting adaptive internetwork interactions.

Qifu Li, Siwen Zhao, and Gaoyangzi Huang contributed equally to this study and shared first authorship.

© 2025 The Obesity Society.

Obesity, 2025; 0:1–13 https://doi.org/10.1002/oby.70040

Study Importance

- What is already known?
 - Appetite dysregulation contributes significantly to the development of abdominal obesity (AO), and individuals with AO exhibit varying appetite levels, such as moderate (MA) and strong appetite (SA).
- Functional connectivity (FC) alterations in brain networks, including the default mode network (DMN), have been linked to obesity and eating behavior in resting-state studies, but little is known about how these neural changes differ across appetite subtypes in AO.
- Why does this study add?
 - This study identifies distinct patterns of brain network disruptions in MA and SA subtypes of female AO using resting-state fMRI.
- SA is characterized by more widespread reduced FC in the DMN, frontoparietal network (FPN), and visual network, as well as lower angular gyrus connectivity, while MA exhibits selective FC reductions and increased internetwork connectivity (DMN-FPN).
- These alterations show subtype-specific correlations with obesity indicators, such as negative associations in SA with BMI and appetite visual analog scale scores.
- How might these results change the direction of research or the focus of clinical practice?
 - By revealing neuro-functional differences between appetite subtypes, including their correlations with obesity measures, this study suggests that individualized treatments targeting specific brain networks—particularly those linked to cognitive control and visual processing—may improve appetite regulation and obesity management.
 - These findings lay the groundwork for brainbased subtyping of AO and support the development of personalized, neurobiologically informed interventions.

1 | Introduction

Abdominal obesity (AO), a chronic metabolic disorder characterized by visceral adipose tissue overaccumulation, poses greater health risks than general obesity [1]. In China, epidemiological data in China in 2020 indicate that the prevalence of AO among middle-aged women reached 34.08%, significantly higher than that in men [2]. Over the past two decades, female AO rates have surged from 19.84% to 43.15%, establishing it as a predominant metabolic threat to women's health [3]. Beyond its associations with cardiovascular diseases, type 2 diabetes, and cancers (such as breast and colon cancer) [4-6]. AO in women also notably increases the risks of polycystic ovary syndrome, reproductive dysfunction, and estrogen-dependent tumors [7]. Hormonal fluctuations and metabolic susceptibilities further exacerbate women's vulnerability to these complications, highlighting the urgent need for targeted interventions in this population [8].

Appetite regulation is central to energy homeostasis, involving dynamic coordination between central reward circuits and peripheral metabolic signals. Recent research identifies D1 medium spiny neurons (D1-MSNs) in the nucleus accumbens (NAc) shell as key mediators of leptin's anorexigenic effects, suppressing appetite via glutamatergic projections to leptin receptor-expressing neurons in the lateral hypothalamus [9]. This circuit integrates homeostatic feeding with hedonic reward systems. In AO, this regulation is disrupted—appetite becomes dissociated from physiological demand and increasingly influenced by hedonic craving [10, 11]. Gender-specific factors, such as blunted satiety responses and preferential abdominal fat deposition linked to estrogenic modulation of NAc-hypothalamic connectivity, amplify these effects in women [12, 13].

Neuroimaging studies reveal a hierarchical framework for appetite regulation, with the hypothalamus governing homeostatic aspects [14, 15], and the limbic system contributing to reward-driven behaviors [16]. Higher-order modulation of food reward valuation involves interactions between the default mode network (DMN), implicated in self-referential thinking and emotional regulation, and the frontoparietal network (FPN), crucial for cognitive control and goal-directed behavior [17]. While task-based studies demonstrate dynamic cross-network interactions during appetite-related processes [18], resting-state functional magnetic resonance imaging (rs-fMRI) uncovers intrinsic connectivity patterns that may underlie these mechanisms, providing insights into baseline network organization without external stimuli [18, 19].

Clinically, our prior work identified two distinct appetite subtypes in AO: moderate appetite (MA) and strong appetite (SA) phenotypes [20]. Notably, these subtypes exhibit not only differential treatment responses, with SA showing better outcomes to interventions like acupoint catgut embedding [20, 21], but also distinct behavioral profiles. MA is characterized by milder appetite drives (VAS scores 4-6), potentially allowing for better self-regulation of intake, whereas SA features heightened appetite intensity (VAS scores 7-10), associated with increased hedonic hunger, compulsive eating, and poorer inhibitory control over food cues [10, 19]. This behavioral divergence prompts the question: Do MA and SA subtypes display unique patterns of functional network reorganization, particularly in DMN/FPN connectivity linked to NAc-hypothalamic circuits, that explain variations in appetite behaviors and treatment responsiveness?

Traditional region-of-interest (ROI) analyses often overlook large-scale network dynamics in appetite control. To address this, we employed independent component analysis (ICA) on rs-fMRI data. ICA is a data-driven approach that identifies resting-state networks (RSNs) and their functional connectivity (FC) without predefined regions [22, 23]. ICA enables unbiased whole-brain exploration of intranetwork FC and internetwork functional network connectivity (FNC), ideal for revealing subtype-specific alterations [18]. Building on the behavioral and clinical differences between MA and SA [20, 21], this study aimed to elucidate the neural underpinnings of these phenotypic variations. Specifically, we investigated whether MA and SA individuals demonstrate distinct FC patterns

within and between key RSNs. Furthermore, we explored the association between these network alterations (distinct FC and FNC patterns in key RSNs) and obesity-related indices, such as body mass index (BMI) and waist circumference (WC). By elucidating the neural signatures, this study aimed to advance mechanistic insights into hedonic appetite regulation and inform personalized, neurobiologically targeted interventions for female AO.

2 | Methods

2.1 | Study Design

This cross-sectional investigation utilized baseline data from an ongoing clinical neuroimaging trial. All participants provided written informed consent before undergoing study-related procedures. The rs-fMRI data were acquired from all participants, and ICA was implemented to identify both intranetwork FC and internetwork FNC across brain networks. The study protocol received ethical approval from the Medical Ethics Committee of the Sports Trauma Specialist Hospital of Yunnan Province (Approval No. 2021-01) and was prospectively registered with the Chinese Clinical Trial Registry (Registration No. ChiCTR2100048920). The trial registration was submitted on July 19, 2021, with the first participant formally enrolled on August 9, 2021.

2.2 | Participants

From August 2021 to June 2024, a total of 60 female patients with AO (comprising 30 with MA and 30 with SA) and 30 female healthy controls (HCs) were recruited from the Second Affiliated Hospital of Yunnan University of Chinese Medicine, the Sports Trauma Specialist Hospital of Yunnan Province, and the Kunming communities in China. The diagnostic criteria were based on the guidelines established by the 2011 Chinese Expert Consensus on the Prevention and Treatment of Adult Obesity [24] and the characteristics of AO [25]. Inclusion criteria for AO included: (1) BMI \geq 28 kg/m² and WC \geq 80 cm; (2) female, right-handed, aged 18-40 years old; (3) appetite stratification using visual analog scale (VAS) scores: MA group (4-6 points) and SA group (7-10 points) based on established cutoffs [20]; (4) at least 6 years of education, with the ability to comprehend the study procedures. Exclusion criteria were: (1) extreme obesity (BMI \geq 40 kg/m²); (2) secondary obesity due to endocrine diseases (e.g., hypothalamic diseases, gonadal disorders, Cushing's syndrome, pituitary disorders, thyroid disorders) or medications (e.g., antipsychotics, glucocorticoid) used; (3) current pregnancy/lactation; (4) comorbidities such as diabetes, cardiovascular disease, psychiatric disorders, immune deficiencies, hepatic or renal impairments, and hematological disorders; (5) psychiatric symptoms, including depression or insomnia; (6) MRI contraindications (e.g., metal implants, vascular stents, pacemakers, dentures, claustrophobia); (7) structural brain abnormalities or cranial asymmetry; (8) history of bariatric surgery. Concurrently, 30 age-matched female HCs were enrolled with normal BMI $(18.5-23.9 \text{ kg/m}^2)$ and MA (VAS scores 4-6), while sharing identical exclusion criteria with AO patients except for obesity-related parameters.

2.3 | Sample Size Calculation

The objective of our study was to identify FC and networklevel differences between MA and SA subtypes in female AO. To ensure sufficient statistical power, the sample size was calculated based on a prior obesity-related FC study [19], which demonstrated significant group differences in FNC between the salience network (SN) and the FPN, with t values of -3.937(SN-IFPN, p=0.0002) and -2.953 (SN-rFPN, p=0.0043) in a sample of 35 participants with obesity and 35 normal-weight participants, corresponding to an average effect size of Cohen's d=0.83. To adopt a conservative approach and account for potential variability in our subtype-specific comparisons, we used Cohen's d=0.8. The required sample size was estimated using PASS software (https://www.ncss.com/software/pass), assuming a two-tailed test, $\alpha = 0.05$, and power = 0.9. This calculation indicated approximately 21 participants per group. To ensure adequate power and allow for potential data exclusions, we included 60 AO patients (30 MA, 30 SA) and 30 HCs, resulting in a total sample of 90 participants.

2.4 | MRI Data Acquisition

Neuroimaging data were acquired using a 3.0T GE Discovery 750w MRI system (GE Healthcare) equipped with a 32-channel head coil for improved signal to noise ratio. During scanning, participants were positioned supine with foam padding around the head to minimize motion artifacts and wore noise-reduction earplugs to attenuate scanner noise. Standardized instructions were provided to all participants to ensure consistency: maintain wakefulness throughout the scan, keep eyes closed without exposure to visual stimulation, breathe relaxedly, and avoid any structured cognitive activities. High-resolution 3D T1-weighted BRAVO images were acquired with the following parameters: repetition time (TR) = 7.7 ms, echo time (TE) = 3.6 ms, matrix = 228×228 , field of view (FOV) = 250×250 mm, 230 axial slices, and acquisition time = 6 min 53 s. The rs-fMRI data were acquired using a gradient recalled echo-echo planar imaging (GRE-EPI) sequence with the following parameters: $TR = 2000 \,\text{ms}$, TE = 30 ms, matrix = 64×64 , $FOV = 220 \times 220 \text{ mm}$, 30 slices, slice thickness = 4.0 mm, gap = 1.2 mm, flip angle = 90°, 240 functional volumes, and acquisition time = 8 min 6 s. Scanning protocols included real-time motion monitoring, with immediate termination upon participant-reported discomfort or excessive head movement (translation > 2 mm, rotation > 2°).

2.5 | Data Processing

2.5.1 | Preprocessing

The rs-fMRI data were preprocessed using the GRETNA toolbox (v2.0.0, http://www.nitrc.org/projects/gretna) in MATLAB R2018b (MathWorks Inc.). The preprocessing steps were as follows: (1) conversion of raw DICOM files to NIFTI format; (2) removal of the first 10 time points to ensure signal stabilization; (3) slice-timing and head motion realignment, with exclusion of participants exhibiting > 2 mm translation or > 2°

Obesity, 2025 3

rotation correction (exclusion threshold: head motion > 2 mm): (4) spatial normalization to Montreal Neurological Institute (MNI) space (voxel size = $3 \times 3 \times 3 \text{ mm}^3$); (5) spatial smoothing with an 8 mm full-width at half-maximum (FWHM) Gaussian kernel; (6) band filtering (0.01-0.08 Hz) to reduce lowfrequency drift and high-frequency noise; and (7) nuisance signal regression to remove non-neural signals. Nuisance regressors included mean signals from white matter (WM) and cerebrospinal fluid (CSF), extracted using masks derived from MNI templates, and head motion parameters modeled with the Friston 24-parameter approach (six motion parameters, their first derivatives, and squared terms). Global signal regression (GSR) was not applied to preserve intrinsic FC patterns, as GSR may remove neural-related signals and introduce artifacts [26]. Framewise displacement (FD) was calculated using the six-dimensional time-series method [27]. All participants had > 90% valid volumes. Following these steps, the preprocessed data from all participants were prepared for further analysis (Figure 1).

2.5.2 | ICA

Group-level spatial ICA was performed using the Group ICA of fMRI Toolbox (GIFT, v4.0b, http://mialab.mrn.org/software/gift) in MATLAB R2018b. To enable unified analysis across all three groups (MA, SA, HC), ICA was conducted on the combined dataset of 90 participants, with the number of independent components (ICs) automatically estimated using the minimum description length (MDL) criterion, which balances model complexity and data fit, yielding 26 components for the overall group analysis. Dimensionality reduction was achieved

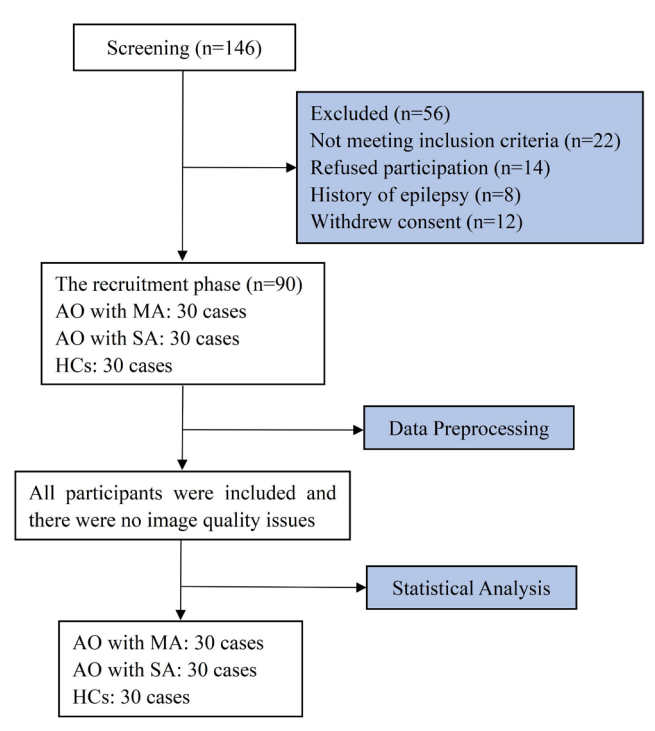


FIGURE 1 | Flowchart of participants' inclusion and exclusion process. HC, healthy control; MA, moderate appetite; SA, strong appetite.

through three stages of principal component analysis (PCA) to compress the data while retaining variance. ICA decomposition was conducted using the Infomax algorithm with extended stability testing: 100 iterations using the ICASSO framework (v1.0, http://research.ics.aalto.fi/ica/icasso) to assess component reliability. A cluster quality index (I_q) threshold>0.9 was applied to ensure stable components, and the maximum number of iterations was set to 512 for convergence. Individual participant spatial maps and temporal dynamics were reconstructed via the group ICA back-reconstruction algorithm (GICA3), preserving between-subject variability while maintaining group-level correspondence.

2.5.3 | Identification of RSNs

The ICs associated with cerebrospinal fluid, motion, or vascular-induced pseudo hyperactivity were discarded based on the graphical user interface display window showing all components in the GIFT toolbox. The spatial correlation coefficient of each IC with the network template was calculated according to the maximum spatial similarity principle of Stanford's Functional Imaging in Neuropsychiatric Disorders (FIND) Laboratory template. ICs corresponding to the maximum correlation coefficient were then identified and combined with manual visual observation to identify and extract brain networks. All ICs were comparatively checked by two independent neuroradiologists to ensure the correctness and appropriateness of the RSNs selection. The eight RSNs included: auditory network (AUN), DMN, dorsal attention network (DAN), ventral attention network (VAN), left FPN (FPN_L), right FPN (FPN_R), sensorimotor network (SMN), and visual network (VN), as illustrated in Figure 2.

2.5.4 | Functional Connectivity Analysis

FC analyses were implemented through a two-stage protocol in MATLAB SPM12. First, within-network connectivity was assessed using one-sample t tests to establish baseline network integrity across all participants, providing a reference for group comparisons. To identify regions of overall group differences, one-way ANOVA was initially applied to generate a mask of significant voxels (F test p < 0.05, FDR-corrected, to balance sensitivity and control for false positives in multigroup comparisons), followed by post hoc two-sample t tests within this mask for pairwise contrasts (MA vs. HC, SA vs. HC, SA vs. MA) with two-tailed testing, incorporating age as a nuisance covariate (FWE-corrected, voxel p < 0.001, cluster p < 0.05). For internetwork FNC, time series of RSNs were extracted, using the Mancovan module in the GIFT toolbox. These time series were Fisher z-transformed and correlated to construct individual FNC matrices. Group differences in FNC were assessed using one-way ANOVA to generate a mask of significant RSN pairs (F test p < 0.05), followed by post hoc t tests, with FDR correction (p < 0.05, Benjamini-Hochberg method [28]) applied to control for multiple comparisons across RSN pairs. FDR was chosen for FNC to balance statistical sensitivity and control of false discoveries in ROI-to-ROI connectivity analyses.

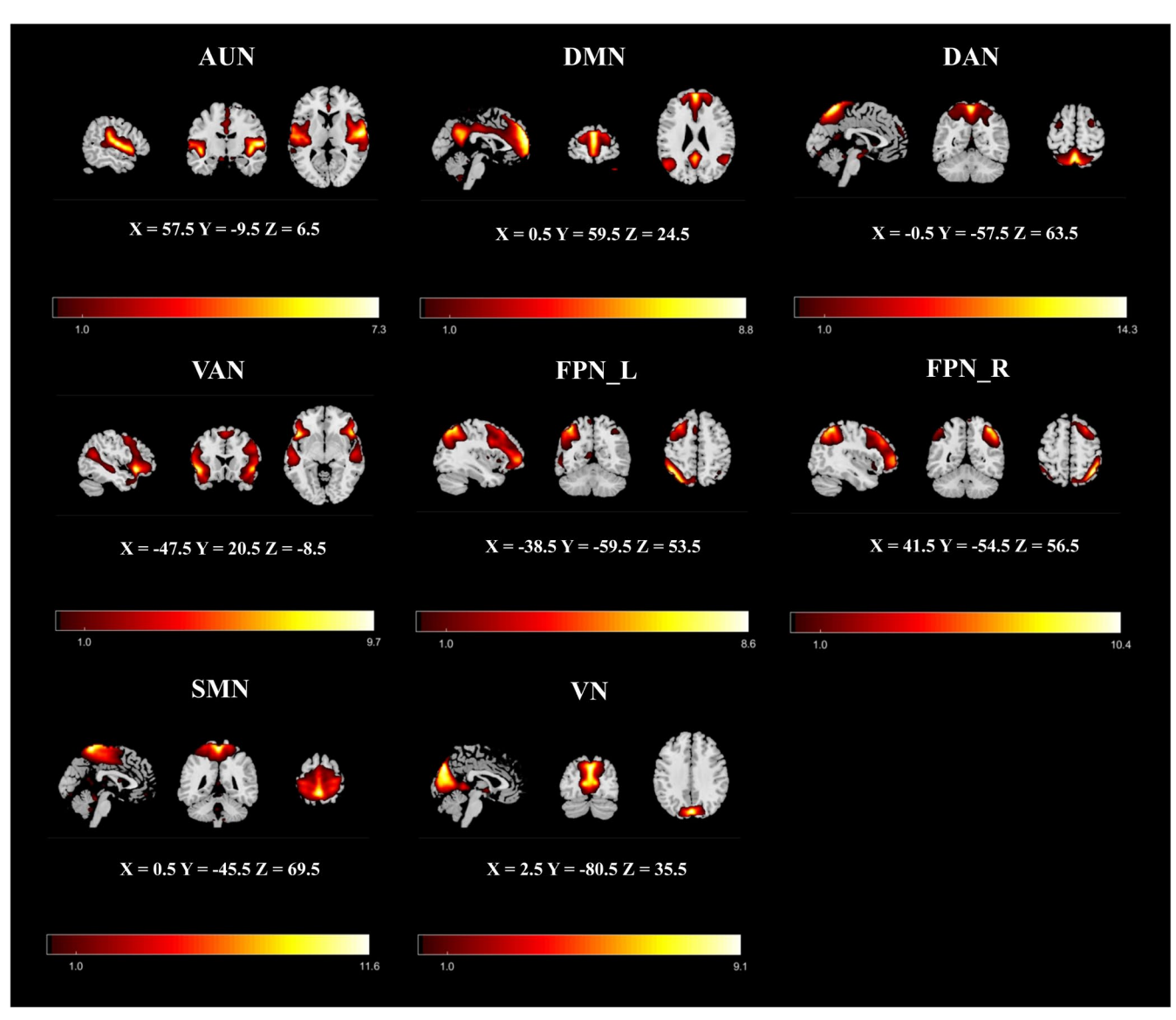


FIGURE 2 | Functional brain network components. AUN, auditory network; DAN, dorsal attention network; DMN, default mode network; FPN_L, left frontoparietal network; FPN_R, right frontoparietal network; SMN, sensorimotor network; VAN, ventral attention network; VN visual network.

2.6 | Statistical Analysis

Demographic and clinical characterization was conducted in SPSS 27.0 statistical software (SPSS Inc.). Continuous variables with normal distribution were expressed as mean \pm standard deviation (SD) and analyzed with parametric methods: independent samples t tests for two-group comparisons and one-way ANOVA with least significant difference (LSD) post hoc tests for three-group contrasts. Non-normally distributed variables were presented as median (interquartile range) and assessed with nonparametric tests: Mann-Whitney U or Kruskal-Wallis with Dunn's post hoc for three groups. Categorical data were described using frequency count (percentage) and analyzed with χ^2 tests. Correlation analyses between clinical variables (e.g., BMI, WC, appetite VAS scores) and neuroimaging metrics (FC values or FNC matrices) were performed using Pearson correlation. Bonferroni correction was applied for multiple comparisons, with statistical

significance set at $p \times n < 0.05$, where n represents the number of tests.

3 | Results

3.1 | Demographics and Clinical Characteristics

The demographics and clinical characteristics of the participants are presented in Table 1. There were no significant differences in age among the MA, SA, and HC groups (p>0.05). However, body weight (BW), WC, and BMI were significantly higher in the SA and MA groups compared to the HC group (p<0.001). No significant differences were observed between the MA and SA groups in terms of BW and BMI (p>0.05). However, the SA group exhibited a significantly longer disease duration, higher WC, and elevated appetite VAS scores than the MA group (p<0.05).

Obesity, 2025 5

TABLE 1 | Demographic and baseline clinical characteristics of the study population.

Clinical				Baseline	group differ	ences-p
variable	MA(n=30)	SA(n=30)	HC $(n=30)$	MA vs. HC	SA vs. HC	MA vs. SA
Age (years)	32.03 ± 6.35	29.37 ± 5.12	32.40 ± 6.92	0.818	0.060	0.978
Duration of disease (years)	6.50 (3.88, 9.62)	5.00 (3.30, 6.43)	_	_	_	0.034
BW	74.08 ± 5.06	77.06 ± 7.25	55.60 ± 4.62	< 0.001	< 0.001	0.070
BMI	28.84 (28.4, 30.27)	29.55 (28.57, 31.79)	29.55 (20.17, 23.17)	< 0.001	< 0.001	0.162
WC	95.75 (91.00, 98.75)	99.25 (94.75, 108.10)	77.50 (76.00, 78.00)	< 0.001	< 0.001	0.009
Appetite VAS score	6.00 (5.00, 6.00)	8.00 (8.00, 9.00)	5.00 (4.00, 6.00)	0.096	< 0.001	< 0.001

Note: Data given as mean \pm SD and median (quartiles). The p value was obtained by the independent t test.

Abbreviations: BW, body weight; HC, healthy control; MA, moderate appetite; SA, strong appetite; VAS, visual analog scale; WC, waist circumference.

3.2 | FC/FNC Within and Between RSNs

Pearson correlation coefficients were computed for the eight RSNs in the MA, SA, and HC groups to construct the FNC matrix.

3.3 | Intranetwork FC Variations

Significant differences in intranetwork FC were observed among the groups based on one-way ANOVA followed by post hoc tests (p < 0.05, FDR-corrected) (Table 2 and Figure 3). Compared with the HC group, both the MA and SA groups demonstrated decreased FC within multiple RSNs, with SA showing more widespread and pronounced reductions. In the MA group, decreased FC was observed in the following regions compared to HCs (post hoc, p < 0.05): DMN: left precuneus (PCUN.L, p < 0.001), right posterior cingulate gyrus (PCG.R, p < 0.001); and VN: left superior occipital gyrus (SOG.L, p < 0.001), right calcarine fissure and surrounding cortex (CAL.R, p < 0.001), left calcarine fissure and surrounding cortex (CAL.L, p < 0.001). In the SA group, decreased FC was observed in the following regions compared to HCs (post hoc p < 0.05): DMN: right posterior cingulate gyrus (PCG.R, p = 0.008), right angular gyrus (ANG.R, p < 0.001); FPN_L: left angular gyrus (ANG.L, p < 0.001), left inferior parietal lobule (IPL.L, p = 0.002); and VN: left superior occipital gyrus (SOG.L, p = 0.024), CAL.L (p = 0.038). Compared to the MA group, the SA group exhibited decreased FC in the following regions (post hoc p < 0.05): DMN: right angular gyrus (ANG.R, p = 0.039); FPN_L: left angular gyrus (ANG.L, p = 0.011), left inferior parietal gyrus (IPL.L, p = 0.016); FPN_R: right superior frontal gyrus, dorsolateral (SFGdor.R, p = 0.004); and VN: right calcarine fissure and surrounding cortex (CAL.R, p = 0.010).

3.4 | FNC Variation Between RSNs

Group comparisons revealed significant FNC differences between the MA and HC groups (p<0.05, FDR-corrected) (Figure 5a,b). The MA group exhibited significantly higher FNC

between the DMN and FPN_L compared to the HC group (95% CI, 0.71 to 0.27, p < 0.001) (Figure 5c).

3.5 | Correlation Analysis

Intranetwork correlation: In the MA group, FC in the VN was positively correlated with WC (r=0.0.4737, p=0.0082×4<0.05) (Figure 4). In the SA group, FPN_L FC was negatively correlated with BMI and DMN (r=-0.3840, p=0.0362<0.05) and appetite VAS (r=-0.5604, p=0.0013×4<0.05) (Figure 4). VN FC was negatively correlated with BW (r=-0.4728, p=0.0083×4<0.05), BMI (r=-0.5136, p=0.0037×4<0.05), and appetite VAS (r=-0.4478, p=0.0131<0.05) (Figure 4). Internetwork correlation: In the HC group, FNC between the DMN and FPN_L was positively correlated with BMI (r=0.4549, p=0.0116×4<0.05), while no significant correlation was observed in the MA group (r=-0.1829, p>0.05) (Figure 5d).

4 | Discussion

This study identified significant differences in intranetwork and internetwork functional connectivity (FC and FNC) across female AO patients with MA and SA levels. Both the SA and MA groups demonstrated widespread FC reductions compared to the HC group, particularly within the DMN, VN, and FPN. Notably, the SA group exhibited more pronounced FC disruptions than the MA group, highlighting distinct neural mechanisms underlying different appetite subtypes in AO.

4.1 | DMN Alterations: Implications for Emotional and Cognitive Regulation in AO Subtypes

The DMN plays a crucial role in self-referential thinking and emotional regulation, involving introspection and decision-making processes [29]. In this study, reduced DMN FC was observed in both the MA (PCUN.L, PCG.R) and SA (PCG.R, ANG.R) groups compared to HCs, with SA showing additional reductions in ANG.R relative to MA. Consistent with other

1930/739x, 0, Downloaded from https://oninelibrary.wiley.com/doi/10.1002/oby.70040 by Shalamar Medical & Dental College, Wiley Online Library on [24/10/2025]. See the Terms and Conditions (https://oninelibrary.wiley.com/erms-and-conditions) on Wiley Online Library for rules of use; OA articles are governed by the applicable Creative Commons License

TABLE 2 | Brain regions with significant differences in FC within RSNs.

					MNI				- B	Post hoc test (p)		
RSNs	HEM	Regions	Cluster size	×	Y	Z	Statistical value	p(F)	MA vs. HC	SA vs. HC	MA vs. SA	Group comparison
DMN	Left	PCUN.L	28	-15	09-	33	4.42	< 0.001	<0.001	0.051	0.058	MA <hc< td=""></hc<>
				-15	99-	39	3.45					
				9-	69-	39	3.24					
	Right	PCG.R	19	9	-36	30	4.29	< 0.001	<0.001	0.008	0.211	MA, SA < HC
		ANG.R	18	39	-54	30	4.80	< 0.001	0.108	< 0.001	0.039	SA <ma<hc< td=""></ma<hc<>
FPN_L	Left	ANG.L	15	-39	-63	45	3.72	< 0.001	0.068	< 0.001	0.011	SA <ma<hc< td=""></ma<hc<>
				-33	09-	33	3.39					
	Left	IPL.L	39	-45	-39	39	4.07	< 0.001	0.491	0.002	0.016	SA <ma<hc< td=""></ma<hc<>
				-39	-48	51	3.49					
FPN_R	Right	SFGdor.R	18	27	30	51	3.89	< 0.001	0.764	0.002	0.004	SA <ma<hc< td=""></ma<hc<>
				30	18	51	3.77					
N	Left	SOG.L	38	-15	-81	6	5.36	0.001	<0.001	0.024	0.262	MA, SA < HC
				9-	-87	6	3.62					
				-24	69-	6	3.33					
		CAL.L	42	-3	06-	6	4.83	0.001	< 0.001	0.038	0.113	MA, SA < HC
				-12	06-	3	3.68					
	Right	CAL.R	16	18	-72	12	4.07	< 0.001	< 0.001	0.306	0.010	MA <hc MA<sa< th=""></sa<></hc

Abbreviations: ANG.L, left angular gyrus; ANG.R, right angular gyrus; CAL.L, left calcarine fissure and surrounding cortex; CAL.R, right calcarine fissure and surrounding cortex; DMN, default mode network; FPN_L, left inferior parietal network; FPN_R, right frontoparietal network; HC, healthy control; HEM, hemisphere: IPL.L, left inferior parietal gyrus; MA, moderate appetite; MNI, Montreal Neurological Institute; PCG.R, right posterior cingulate gyrus; PCUN.L, left precuneus; SA, strong appetite; SFGdor.R, right superior frontal gyrus, dorsolateral; SOG.L, left superior occipital gyrus; VN, visual network.

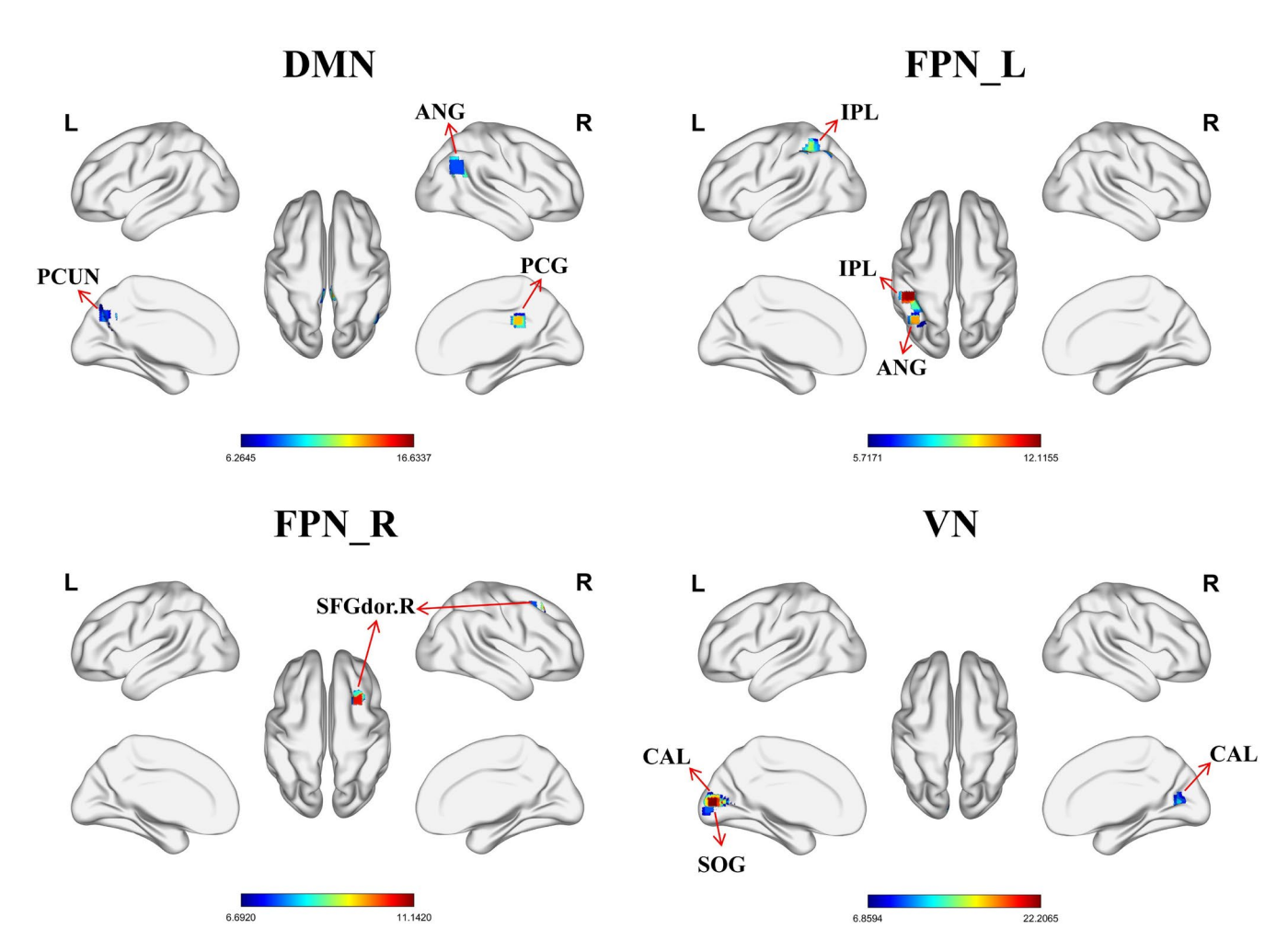


FIGURE 3 | Differences in FC within resting-state networks. Brain regions with significant FC differences within resting-state networks were observed in the DMN, FPN_L, FPN_R, and VN. The color bar indicates *t*-statistics, with warmer colors highlighting regions of stronger statistical significance (*p* < 0.05, FDR-corrected). ANG, angular gyrus; CAL, calcarine fissure and surrounding cortex; DMN, default mode network; FPN_L, left frontoparietal network; FPN_R, right frontoparietal network; IPL, inferior parietal gyrus; PCG, posterior cingulate gyrus; PCUN, precuneus; SFGdor.R, right superior frontal gyrus, dorsolateral; SOG, superior occipital gyrus; VN, visual network.

rs-fMRI studies, individuals with obesity exhibit decreased DMN FC, particularly in the posterior cingulate cortex, PCUN, and ANG, which has been shown to correlate with higher BMI and impaired self-regulatory processing in individuals with obesity [30, 31]. For instance, a meta-analysis of rs-fMRI in obesity found reduced DMN connectivity associated with emotional regulation deficits and poorer inhibitory control, without external stimuli [30]. The more severe DMN reductions in SA, including the ANG.R (involved in attention and memory integration), may indicate heightened vulnerability to selfregulation challenges, as supported by rs studies showing DMN FC decreases correlating with increased appetite drives [19, 31]. This subtype difference is further supported by SA's longer disease duration and higher VAS scores, which may relate to these reductions, as rs-fMRI in obesity links angular gyrus FC decreases to elevated appetite behaviors [19]. In contrast, the relatively milder reductions in MA suggest a less disrupted introspective network, consistent with patterns observed in rsfMRI of obesity cohorts after weight loss interventions, where DMN activity increases correlate with improved metabolic outcomes [32].

4.2 | VN Alterations: Implications for Visual Processing in AO Subtypes

In this study, significant FC reductions in the VN were observed in both the MA and SA groups, particularly in regions like the CAL and SOG. In MA, VN FC was positively correlated with WC, while in SA, it was negatively correlated with BW, BMI, and appetite VAS scores. These opposing correlations highlight subtype-specific associations between VN connectivity and obesity measures. Rs-fMRI studies in obesity consistently report VN disruptions, with decreased FC in visual processing areas linked to altered reward sensitivity and higher BMI [33, 34]. The negative correlations in SA suggest that VN reductions may exacerbate appetite drives, consistent with rs-fMRI findings of increased temporal variability in visual regions correlating with BMI [34]. This is further supported by SA's higher VAS scores and longer disease duration, which may relate to these VN alterations. In contrast, the positive correlation in MA indicates a potentially different mechanism, where preserved or heightened VN activity could reflect compensatory visual processing, aligning with subtypespecific rs patterns observed in overweight individuals [35].

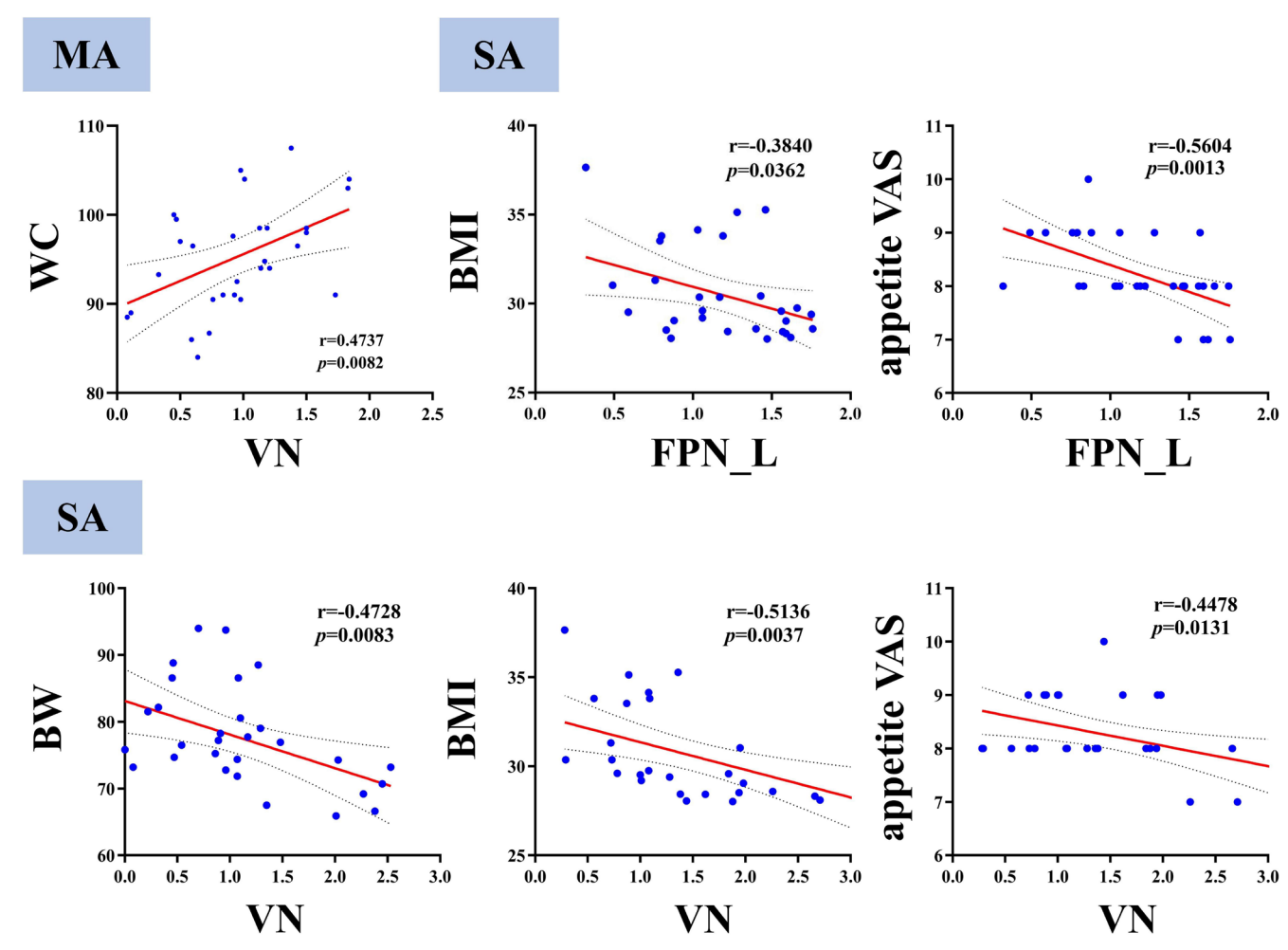


FIGURE 4 Analysis of intranetwork functional connectivity correlations. BW, body weight; FPN_L, left frontoparietal network; MA, moderate appetite; SA, strong appetite; VAS, visual analog scale; VN, visual network; WC, waist circumference.

4.3 | FPN Reductions: Implications for Cognitive Control in the SA Subtype

The FPN, essential for cognitive control and goal-directed behavior [36], showed significantly reduced FC in the SA group compared to both the HC and MA groups, particularly in the ANG.L, IPL.L (FPN_L), and SFGdor.R (FPN_R). In SA, FPN_L FC was negatively correlated with BMI and appetite VAS, underscoring potential links to obesity severity and eating behaviors. A study of individuals with obesity reported disrupted FPN FC at rest, correlating with poor decision-making [19]. The preserved FPN FC in MA, contrasted with SA's reductions and negative correlations, suggests that cognitive control mechanisms may remain relatively intact in MA, consistent with rs-fMRI evidence of FPN-BMI relationships in appetite-related disorders [37]. This subtype difference is further supported by SA's higher VAS scores, which may relate to these FPN reductions, as the rs-fMRI study noted that weaker FPN connectivity was significantly associated with higher disinhibited eating scores, reinforcing the link between FPN integrity and maladaptive eating behaviors [17]. These findings suggest that targeting FPN functionality through cognitive-behavioral interventions may be particularly beneficial for SA patients.

4.4 | FNC Patterns: Implications for Network Interactions in AO Subtypes

Internetwork connectivity analysis revealed increased FNC between the DMN and FPN L in the MA group compared to HCs, with positive DMN-FPN_L FNC correlations with BMI in HCs but absent in MA. This heightened interaction in MA, without similar patterns in SA, may reflect adaptive network coupling to support appetite regulation [38]. Rs studies in obesity show altered DMN-FPN interactions, with increased FNC potentially compensating for regulatory challenges, as seen in correlations with behavioral measures like BMI [34, 39]. For instance, rsfMRI in overweight individuals demonstrated enhanced DMN-FPN FNC linked to better weight management outcomes [19]. In contrast, the lack of compensation in SA aligns with their more severe FC reductions and negative correlations, supporting rsfMRI findings of disrupted internetwork dynamics in advanced obesity [39]. This is further supported by SA's higher VAS scores and greater disease burden, which may relate to these FNC absences, as rs-fMRI evidence in obesity shows DMN-FPN decoupling correlating with elevated appetite and maladaptive behaviors [19].

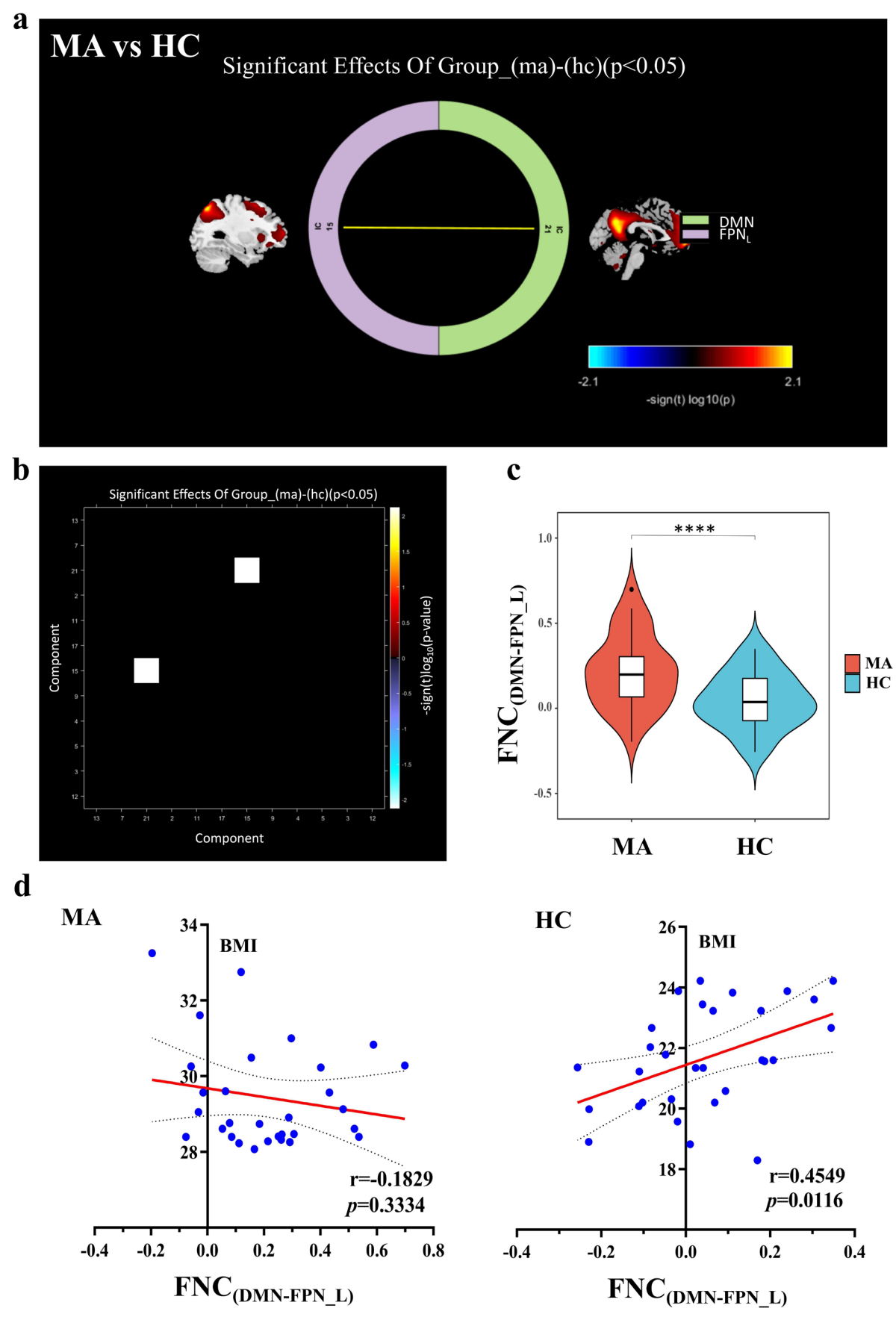


FIGURE 5 | Legend on next page.

FIGURE 5 | Functional network connectivity differences between MA and HC groups. (a) Ring diagram illustrating increased connectivity between the DMN and FPN_L in the MA group compared to the HC group. The color bar represents log-transformed p values (log10), with positive values indicating stronger connectivity in the MA group. (b) Matrix plot showing significant FNC differences between RSNs. Yellow squares represent significant FNC differences (p<0.05, FDR-corrected), with warmer colors indicating increased connectivity in the MA group. (c) FNC between the DMN and FPN_L is significantly higher in the MA group. (d) Analysis of internetwork functional network connectivity correlations. DMN, default mode network; FNC, functional network connectivity; FPN_L, left frontoparietal network; HC, healthy control; MA, moderate appetite; SC, strong appetite.

4.5 | Clinical Implications and Translational Potential

The observed FC and FNC alterations, particularly their correlations with obesity indicators, offer critical insights for clinical applications. In the SA group, pronounced reductions in FPN and VN, negatively correlated with BMI and appetite VAS, underscore the need for interventions targeting cognitive control and sensory processing networks. Real-time fMRI-guided approaches, such as neurofeedback training to upregulate prefrontal activity, have shown promise in improving eating behaviors in overweight individuals by modulating networks like FPN [40]. For the MA group, the increased DMN-FPN_L FNC and positive VN-WC correlations suggest benefits from strategies supporting adaptive interactions, like mindfulness-based interventions that enhance introspection and decision-making [41, 42]. Cognitive-behavioral therapy [43] could be tailored to these functional connections, as rs-fMRI studies indicate it alters DMN-FPN connectivity in obesity [17]. Similarly, mindful eating practices may recalibrate VN responses, with rs evidence linking them to reduced appetite drives and improved weight management [44]. Integrating these with rs-fMRI monitoring could personalize treatments, synergistically enhancing effectiveness for subtype-specific appetite regulation.

This study has several limitations. First, the sample size was relatively small, limiting the generalizability of the findings. Second, the reliance on a single appetite assessment scale may not fully capture the complexity of appetite regulation. Third, the cross-sectional design precludes conclusions about the temporal evolution of FC and FNC alterations in AO. As a rs study, interpretations are inferential and based on correlations; future task-based fMRI (e.g., food-cue paradigms [45]) is needed to validate functional implications. Larger, longitudinal studies with diverse samples and multimodal assessments could further elucidate these patterns.

5 | Conclusion

In summary, this study highlights distinct neural mechanisms underlying appetite subtypes in female AO patients. SA patients exhibited greater disruptions in networks linked to self-regulatory and visual processing, potentially contributing to appetite dysregulation based on negative correlations with obesity indicators like BMI and VAS scores. In contrast, MA patients showed increased DMN-FPN_L interactions, which may reflect adaptive mechanisms to mitigate appetite-related challenges. These findings provide novel insights into understanding the central appetite-related patho-mechanisms of AO and suggest potential targets for personalized

interventions to improve appetite control and weight management in obesity.

Author Contributions

Concept and design: T.G., F.L., and Y.L. Assessment: S.Z., Z.L., and C.X. Acquisition of data: Z.C., X.P., R.Y., R.H., and J.Z. Analysis design: Y.L. and X.T. Drafting of the manuscript: Q.L., S.Z., and G.H. All authors revised and approved the final version of the manuscript. T.G. had full access to all of the data in the study and takes responsibility for the integrity of the data and the accuracy of the data analysis.

Acknowledgments

The authors would like to thank all the participants involved in the study, as well as other staff for their support.

Conflicts of Interest

The authors declare no conflicts of interest.

Data Availability Statement

The data that support the findings of this study are available from the corresponding author upon reasonable request.

References

- 1. D. Dhawan and S. Sharma, "Abdominal Obesity, Adipokines and Non-Communicable Diseases," *Journal of Steroid Biochemistry and Molecular Biology* 203 (2020): 105737.
- 2. W. J. Tu, Z. Zhao, F. Yan, X. Zeng, and J. Li, "Geographic and Ethnicity Variation in the Prevalence of Middle-Aged and Elderly Adult Obesity in China in 2020," *Diabetes, Obesity & Metabolism* 26, no. 5 (2024): 1897–1907.
- 3. Y. Chen, Q. Peng, Y. Yang, S. Zheng, Y. Wang, and W. Lu, "The Prevalence and Increasing Trends of Overweight, General Obesity, and Abdominal Obesity Among Chinese Adults: A Repeated Cross-Sectional Study," *BMC Public Health* 19, no. 1 (2019): 1293.
- 4. A. Fenton, "Weight, Shape, and Body Composition Changes at Menopause," $\it Journal\ of\ Mid-Life\ Health\ 12,$ no. 3 (2021): 187–192.
- 5. T. M. Powell-Wiley, P. Poirier, L. E. Burke, et al., "Obesity and Cardiovascular Disease: A Scientific Statement From the American Heart Association," *Circulation* 143, no. 21 (2021): e984–e1010.
- 6. C. Zhang, K. M. Rexrode, R. M. van Dam, T. Y. Li, and F. B. Hu, "Abdominal Obesity and the Risk of All-Cause, Cardiovascular, and Cancer Mortality: Sixteen Years of Follow-Up in US Women," *Circulation* 117, no. 13 (2008): 1658–1667.
- 7. A. E. Joham, R. J. Norman, E. Stener-Victorin, et al., "Polycystic Ovary Syndrome," *Lancet Diabetes and Endocrinology* 10, no. 9 (2022): 668–680.
- 8. E. Mazza, E. Troiano, Y. Ferro, et al., "Obesity, Dietary Patterns, and Hormonal Balance Modulation: Gender-Specific Impacts," *Nutrients* 16, no. 11 (2024): 1629.

- 9. Y. Liu, Y. Wang, Z. D. Zhao, et al., "A Subset of Dopamine Receptor-Expressing Neurons in the Nucleus Accumbens Controls Feeding and Energy Homeostasis," *Nature Metabolism* 6, no. 8 (2024): 1616–1631.
- 10. S. Wharton, D. C. W. Lau, M. Vallis, et al., "Obesity in Adults: A Clinical Practice Guideline," *CMAJ* 192, no. 31 (2020): E875–e891.
- 11. S. M. Sternson and A. K. Eiselt, "Three Pillars for the Neural Control of Appetite," *Annual Review of Physiology* 79 (2017): 401–423.
- 12. T. Amin and J. G. Mercer, "Hunger and Satiety Mechanisms and Their Potential Exploitation in the Regulation of Food Intake," *Current Obesity Reports* 5, no. 1 (2016): 106–112.
- 13. A. L. Hirschberg, "Sex Hormones, Appetite and Eating Behaviour in Women," *Maturitas* 71, no. 3 (2012): 248–256.
- 14. H. W. Gan, M. Cerbone, and M. T. Dattani, "Appetite- and Weight-Regulating Neuroendocrine Circuitry in Hypothalamic Obesity," *Endocrine Reviews* 45, no. 3 (2024): 309–342.
- 15. H. Alzaid, J. J. Simon, G. Brugnara, P. Vollmuth, M. Bendszus, and H. C. Friederich, "Hypothalamic Subregion Alterations in Anorexia Nervosa and Obesity: Association With Appetite-Regulating Hormone Levels," *International Journal of Eating Disorders* 57, no. 3 (2024): 581–592.
- 16. W. D. Killgore, M. Weber, Z. J. Schwab, et al., "Cortico-Limbic Responsiveness to High-Calorie Food Images Predicts Weight Status Among Women," *International Journal of Obesity (Lond)* 37, no. 11 (2013): 1435–1442.
- 17. A. Brennan, L. Marstaller, H. Burianová, et al., "Weaker Connectivity in Resting State Networks Is Associated With Disinhibited Eating in Older Adults," *International Journal of Obesity (Lond)* 46, no. 4 (2022): 859–865.
- 18. Z. Tan, Y. Hu, G. Ji, et al., "Alterations in Functional and Structural Connectivity of Basal Ganglia Network in Patients With Obesity," *Brain Topography* 35, no. 4 (2022): 453–463.
- 19. Y. Ding, G. Ji, G. Li, et al., "Altered Interactions Among Resting-State Networks in Individuals With Obesity," *Obesity (Silver Spring)* 28, no. 3 (2020): 601–608.
- 20. X. Zhang, Q. Li, R. Yi, et al., "Effect of Acupoint Catgut Embedding for Abdominally Obese Female With Strong Appetite: Mixed Analysis of a Randomized Clinical Trial," *Diabetes, Metabolic Syndrome and Obesity: Targets and Therapy* 15 (2022): 3387–3395.
- 21. X. Tang, G. Huang, Q. Li, et al., "Effect of Acupoint Catgut Embedding on Subjective Appetite in Overweight and Obese Adults With Strong and Moderate Appetite: A Secondary Analysis of a Randomized Clinical Trial," *Diabetes, Metabolic Syndrome and Obesity: Targets and Therapy* 17 (2024): 4573–4583.
- 22. Y. Yi, N. Billor, A. Ekstrom, and J. Zheng, "CW_ICA: An Efficient Dimensionality Determination Method for Independent Component Analysis," *Scientific Reports* 14, no. 1 (2024): 143.
- 23. E. Kropf, S. K. Syan, L. Minuzzi, and B. N. Frey, "From Anatomy to Function: The Role of the Somatosensory Cortex in Emotional Regulation," *Brazilian Journal of Psychiatry* 41, no. 3 (2019): 261–269.
- 24. Obesity Group, Endocrinology Branch, Chinese Medical Association, "Chinese Expert Consensus on the Prevention and Treatment of Adult Obesity," *Chinese Journal of Endocrinology and Metabolism* 27, no. 9 (2011): 711–717.
- 25. W. T. Garvey, J. I. Mechanick, E. M. Brett, et al., "American Association of Clinical Endocrinologists and American College of Endocrinology Comprehensive Clinical Practice Guidelines for Medical Care of Patients With Obesity," *Endocrine Practice* 22, no. S3 (2016): 1–203.
- 26. K. Murphy and M. D. Fox, "Towards a Consensus Regarding Global Signal Regression for Resting State Functional Connectivity MRI," *NeuroImage* 154 (2017): 169–173.

- 27. J. D. Power, K. A. Barnes, A. Z. Snyder, B. L. Schlaggar, and S. E. Petersen, "Spurious but Systematic Correlations in Functional Connectivity MRI Networks Arise From Subject Motion," *NeuroImage* 59, no. 3 (2012): 2142–2154.
- 28. M. E. Glickman, S. R. Rao, and M. R. Schultz, "False Discovery Rate Control Is a Recommended Alternative to Bonferroni-Type Adjustments in Health Studies," *Journal of Clinical Epidemiology* 67, no. 8 (2014): 850–857.
- 29. A. Harikumar, D. W. Evans, C. C. Dougherty, K. L. H. Carpenter, and A. M. Michael, "A Review of the Default Mode Network in Autism Spectrum Disorders and Attention Deficit Hyperactivity Disorder," *Brain Connectivity* 11, no. 4 (2021): 253–263.
- 30. N. Parsons, T. Steward, R. Clohesy, H. Almgren, and L. Duehlmeyer, "A Systematic Review of Resting-State Functional Connectivity in Obesity: Refining Current Neurobiological Frameworks and Methodological Considerations Moving Forward," *Reviews in Endocrine & Metabolic Disorders* 23, no. 4 (2022): 861–879.
- 31. S. D. Donofry, J. M. Jakicic, R. J. Rogers, J. C. Watt, K. A. Roecklein, and K. I. Erickson, "Comparison of Food Cue-Evoked and Resting-State Functional Connectivity in Obesity," *Psychosomatic Medicine* 82, no. 3 (2020): 261–271.
- 32. Y. Zeighami, S. Iceta, M. Dadar, et al., "Spontaneous Neural Activity Changes After Bariatric Surgery: A Resting-State fMRI Study," *Neuro-Image* 241 (2021): 118419.
- 33. G. E. Doucet, N. Rasgon, B. S. McEwen, N. Micali, and S. Frangou, "Elevated Body Mass Index Is Associated With Increased Integration and Reduced Cohesion of Sensory-Driven and Internally Guided Resting-State Functional Brain Networks," *Cerebral Cortex* 28, no. 3 (2018): 988–997.
- 34. Y. Guo, Y. Xia, and K. Chen, "The Body Mass Index Is Associated With Increased Temporal Variability of Functional Connectivity in Brain Reward System," *Frontiers in Nutrition* 10 (2023): 1210726.
- 35. H. Lee, J. Kwon, J. E. Lee, B. Y. Park, and H. Park, "Disrupted Stepwise Functional Brain Organization in Overweight Individuals," *Communications Biology* 5, no. 1 (2022): 11.
- 36. C. Caldinelli and R. Cusack, "The Fronto-Parietal Network Is Not a Flexible Hub During Naturalistic Cognition," *Human Brain Mapping* 43, no. 2 (2022): 750–759.
- 37. H. Cerit, P. Davidson, T. Hye, et al., "Resting-State Brain Connectivity Predicts Weight Loss and Cognitive Control of Eating Behavior After Vertical Sleeve Gastrectomy," *Obesity (Silver Spring)* 27, no. 11 (2019): 1846–1855.
- 38. S. Lee, J. Y. Namgung, J. H. Han, and B. Y. Park, "Alterations in the Functional MRI-Based Temporal Brain Organisation in Individuals With Obesity," *Diabetes, Obesity & Metabolism* 27 (2025): 5135–5146.
- 39. D. Dong, X. Chen, W. Li, et al., "Opposite Changes in Morphometric Similarity of Medial Reward and Lateral Non-Reward Orbitofrontal Cortex Circuits in Obesity," *NeuroImage* 290 (2024): 120574.
- 40. S. H. Kohl, R. Veit, M. S. Spetter, et al., "Real-Time fMRI Neuro-feedback Training to Improve Eating Behavior by Self-Regulation of the Dorsolateral Prefrontal Cortex: A Randomized Controlled Trial in Overweight and Obese Subjects," *NeuroImage* 191 (2019): 596–609.
- 41. R. B. Pepe, G. Coelho, F. D. S. Miguel, et al., "Mindful Eating for Weight Loss in Women With Obesity: A Randomised Controlled Trial," *British Journal of Nutrition* 130, no. 5 (2023): 911–920.
- 42. T. P. Minari, G. M. Araújo-Filho, L. H. B. Tácito, et al., "Effects of Mindful Eating in Patients With Obesity and Binge Eating Disorder," *Nutrients* 16, no. 6 (2024): 884.
- 43. J. Y. Cha, S. Y. Kim, Y. W. Lim, K. H. Choi, and I. S. Shin, "Comparative Effectiveness of Cognitive Behavioral Therapy and Behavioral Therapy in Obesity: A Systematic Review and Network Meta-Analysis,"

Journal of Clinical Psychology in Medical Settings 32, no. 1 (2025): 96-110.

- 44. P. Lattimore, "Mindfulness-Based Emotional Eating Awareness Training: Taking the Emotional out of Eating," *Eating and Weight Disorders* 25, no. 3 (2020): 649–657.
- 45. M. C. M. Wever, F. van Meer, L. Charbonnier, et al., "Associations Between Ghrelin and Leptin and Neural Food Cue Reactivity in a Fasted and Sated State," *NeuroImage* 240 (2021): 118374.